Mechanical Engineering – Scientific Journal, Vol. **41,** No. 1, pp. 59–70 (2023)
Number of article: 665
In print: ISSN 1857–5293
Received: May 8, 2023
On line: ISSN 1857–9191
Accepted: June 7, 2023
UDC: 656.13.052.54:629.3.027.4-526]:[004.942:519.872
https://doi.org/10.55302/MESJ23411665059ch

Original scientific paper

VEHICLE HANDLING ENHANCEMENT EMPLOYING FOUR-WHEEL INDEPENDENT STEERING SYSTEM USING SLIDING MODE CONTROL

Vasko Čangoski, Igor Ǵurkov, Darko Danev, Vase Jordanoska

Institute of Engineering Design, Mechanization and Motor Vehicles,
Faculty of Mechanical Engineering, University "Ss. Cyril and Methodius" in Skopje,
Ruđer Bošković 18, P.O. box 464, MK-1001 Skopje, Republic of North Macedonia
vasko.changoski@mf.edu.mk

A b s t r a c t: The demand for safer vehicle transportation and future automated vehicles will open the possibility for implementation of steer-by-wire (SbW) vehicle steering system. Application of this system would not be exclusive only for the front axle, but for the rear axle as well. Current four-wheel steering (4WS) systems are designed and applied using Ackermann steering geometry. Due to the vehicle designs requirements, an ideal Ackermann geometry is never achieved and steering kinematics may result in two instantaneous centres of rotation during vehicle cornering. To avoid this, a control strategy for a four-wheel independent steering (4WIS) is proposed where the four independently steered wheels attempt to achieve single instantaneous centre of rotation using sliding mode controller (SMC). As a reference model a 2DOF nonlinear vehicle bicycle model is used. The 4WS and 4WIS two-track vehicle models are created using MATLAB/Simulink and tested with manoeuvres defined by the standard ISO 7401.

Key words: 4WIS; sliding mode control; steer-by-wire; Ackermann geometry

ПОДОБРУВАЊЕ НА УПРАВЛИВОСТА КАЈ ВОЗИЛАТА СО СИСТЕМ ЗА НЕЗАВИСНО УПРАВУВАЊЕ НА ЧЕТИРИ ТРКАЛА СО ПРИМЕНА НА СТРАТЕГИЈАТА СО ЛИЗГАЧКА ПОВРШИНА

А п с т р а к т: Потребата од побезбеден транспорт и автоматизирани возила во иднина налага имплементација на системи за управување преку сигнали, без механички врски. Примената на овие системи не би била само кај предната, туку и кај задната оска. Сегашните системи за управување на четирите тркала се конструирани и применети користејќи Акерманова геометрија. Поради конструктивните барања кај возилата, идеалната Акерманова геометрија никогаш не се постигнува и кинематиката на управувачкиот механизам може да резултира со два истовремени пола на ротација при движење на возилото во кривина. За да се избегне тоа, се предлага стратегија на управување со лизгачка површина на систем за независно управување на тркалата, за сите четири тркала да бидат управувани независно со цел да се постигне единствен моментален пол на ротација. Како референтен модел е искористен нелинеарен модел-велосипед на возило со два степена на слобода. Моделите на возилата со управување на четирите тркала и со независно управување на секое тркало се креирани со помош на МАТЛАБ/Симулник и се тестирани со маневри дефинирани согласно со стандардот ISO 7401.

Клучни зборови: систем за независно управување на четири тркала; управување со лизгачка површина; управување преку сигнали; Акерманова геометрија

NOMENCLATURE

a	Distance between instantaneous centre and front axle
a_y	Lateral acceleration
B	Pacejka tire model stiffness factor
b	Distance between instantaneous centre and rear axle
b_f	Front track width
b_r	Rear track width

C Pacejka tire model shape factor
$C_{F\beta}$ Pacejka tire model stiffness
$C_{\alpha f}$ Front wheel cornering stiffness
$C_{\alpha r}$ Rear wheel cornering stiffness
D Pacejka tire model peak factor
d Distance between the instantaneous centre of rotation and vehicle longitudinal axis
d_i Distance between the instantaneous centre of rotation and vehicle inner wheels
d_o Distance between the instantaneous centre of rotation and vehicle outer wheels
E Pacejka tire model curvature factor
e_j Sliding mode error function (j = 1, 2, 3, 4)
F_n Vertical force
F_{nom} Nominal vertical force
F_{yf} Front tire lateral force
F_{yr} Rear tire lateral force
g Gravitational constant
h Distance between link and axle lateral axis
h_c Centre of mass height
I_z Material moment of inertia
i Inertia radius
k Maximum value of the signal that the SMC controller can produce (j = 1, 2, 3, 4)
K 4WS proportional control strategy constant
l Wheelbase
l_f Distance from centre of mass to front axle
l_r Distance from centre of mass to rear axle
$l_{j_{f,r}}$ Front and rear axle link length (j = 1, 2, 3, 4)
m Mass of the vehicle
R Turning radius
s_j Sliding mode surface function (j = 1, 2, 3, 4)
u_j SMC controller output (j = 1, 2, 3, 4)
u_{eq} SMC desired output signal of the controller in stationary conditions
V_x Longitudinal velocity
V_y Lateral velocity
α_f Front wheel side slip-angle
α_{fi} Front inner wheel side slip-angle
α_{fo} Front outer wheel side slip-angle
α_{fref} Reference front wheel side-slip angle
α_r Rear wheel side-slip angle
α_{ri} Rear inner wheel side-slip angle
α_{ro} Rear outer wheel side-slip angle
α_{rref} Reference rear wheel side-slip angle
β_c Side slip angle
δ_f Front steering steered angle
δ_{fi} Front inner steered wheels angle
δ_{fo} Front outer steered wheels angle
δ_{fref} Reference front steered wheel angle
δ_r Rear steered wheels angle
δ_{ri} Rear inner steered wheels angle
δ_{ro} Rear outer steered wheels angle
δ_{rref} Reference rear steered wheel angle
$\gamma_{j_{f,r}}$ Front and rear axle angle between links
λ Constant which multiplies the error in SMC controller
ϕ Thickness of the boundary layer of the sliding surface in SMC controller
φ Road surface friction coefficient
ω_z Vehicle yaw rate

1. INTRODUCTION

Increased demands for improved overall vehicle performance along with needs for safer and more sustainable transportation lead to development of new advanced vehicle systems.

Regarding vehicle steering system, Ackermann steering geometry is still the most used steering principle in modern vehicles. Beside many advantages, throughout the whole cornering process, the ideal Ackermann geometry with single centre of rotation during turning is rarely achieved. Nevertheless, this principle with mechanical linkage is still used in classic and automated steering systems, such as the Active Front Steering (AFS) and the Active Rear Steering (ARS) in 4WS or AWS vehicles.

Authors in [1] present improved vehicle dynamics and handling by implementing fuzzy-logic controller in coordinated control involving AFS and vehicle yaw control system. Feng *et al.* present coordinated chassis control [2] where the AFS system is integrated with traction control and differen-tial braking. Doumiati *et al.* suggest a phase plane approach [3] that shows improvement in vehicle handling. As AFS control strategy, model predictive control (MPC) is used by Falcone *et al.* [4]. Ding *et al.* suggest sliding mode control (SMC) [5], while authors in [6] combine SMC and extreme learning machine. Another machine learning method is proposed by Huang *et al.* [7] where a neural network controller is implemented.

Authors in [8] present comparison between integrated AFS and vehicle stability control (VSC) and integrated ARS and VSC, controlled by SMC using co-simulation. Hiraoka *et al.* [9] and authors in [8] present the idea of using reference 4WS bicycle model to improve 4WS vehicle performance. In [10] Ferrara presents the application of SMC in broader spectrum of vehicle systems.

Most of the previously mentioned research papers point out the advantages of using AFS and ARS systems which significantly improve the vehicle dynamics. These systems, together with the current type approval legislation requires a mechanical

linkage between the steering wheel and the steered wheels. In order to avoid the disadvantages of the mechanical linkage, many researchers are focused on developing a Steer-by-Wire (SbW) systems. The Steer-by-Wire system would free up more space, lower the weight of the vehicle and most importantly could potentially lead to improved vehicle dynamics and could provide steering correction in case of unwanted driver's command and need to stabilize the vehicle.

In [11] Chen *et al.* propose four-wheel independent steering (4WIS) control strategy based on wheels minimum load. Authors in [12] and [13] present improved vehicle stability of a prototype 4WIS and four-wheel independent driving (4WID) vehicle using several control algorithms. Improved vehicle manoeuvrability is also presented in [14] and [15]. Liu *et al.* present application of SMC in 4WIS system in [16]. Using yaw moment control method, Yim [17] makes a comparison between AFS, front wheel independent steering (FWIS), 4WS and 4WIS. The paper had shown that 4WIS offers the best vehicle performance. Nah and Yim present a combined method between VSC, 4WIS and 4WID [18].

Development of a 4WIS represents state-of-the-art in terms of vehicle steering and handling among researchers and engineers. The application of this system in vehicles would decrease the gap between theoretical and real steering systems performance, thus significantly improving vehicle handling and stability. Unfortunately, the biggest current problem represents the legislation limitations and the lack of redundant mechanism(s) in case of system failure.

To analyze the characteristics and the performance of the 4WIS system, in this paper a nonlinear 4WIS vehicle model is compared with a nonlinear 4WS that uses proportional rear wheel steering control algorithm. As [8] suggests, a reference nonlinear all wheel steering (AWS) bicycle model is created where the rear wheels are steered using linear control strategy to achieve vehicle side-slip angle value of zero in steady and transient state.

This study aims to analyze the potential of the SMC controllers on vehicle stability when employed to generate correction of the desired wheel steer angles in order to achieve single instantaneous centre of rotation. The correction is based on the difference between the wheels steer angles and the wheels side-slip angles because that difference defines the vehicle traveling direction and the cornering radius of the vehicle.

Therefore, by focusing on overcoming the imperfections of mechanical steering mechanism and implementation of SMC controllers in independent all-wheel steering, a control strategy concept is presented which allows more precise determination of the instantaneous centre of rotation, increased vehicle stability, smaller off-tracking and tire deformation.

2. VEHICLE MODELS

The presented concept of 4WIS is based on the aim to achieve single instantaneous centre of rotation, while maintaining the desired wheels' side-slip angles. It would increase vehicle stability, while decreasing tire wearing and loads. As a reference model for the 4WIS, a 2DOF nonlinear bicycle model is used. An additional 4WS model was created, in which both axles have Ackermann steering geometry derived from real vehicle with mechanical linkage. The geometry was chosen because it is still most widely used in passenger vehicles. The effects of implementing four-wheel independent steering are analyzed and presented by comparison between the 4WS and 4WIS vehicle model using standardized test procedures accordingly to the standard ISO 7401.

Figure 1 shows a schematic overview of the proposed concept. The driver commands different front wheel steering angles to both vehicles in order to complete the standardized manoeuvre according to ISO 7401. This is presented in greater details in the results section.

While the front wheel steer angles of the 4WS vehicle depend solely on the driver's command, the final values of the 4WIS front wheel steer angles depend on the driver's command and the correction of the SMC controllers.

On the other hand, the 4WS rear wheels are controlled using a proportional control strategy, while the 4WIS uses control strategy which attempts to achieve vehicle side-slip angle value of zero during steady and transient state. In this case that would not be literally possible because nonlinear vehicle model is being used, while the particular strategy is derived from a linear bicycle model. However, it significantly lowers the values of the vehicle side-slip angle. Beside the input from control strategy, an additional correction is being applied by the SMC controllers. The strategies used and the vehicle models are described in detail in the following subsections.

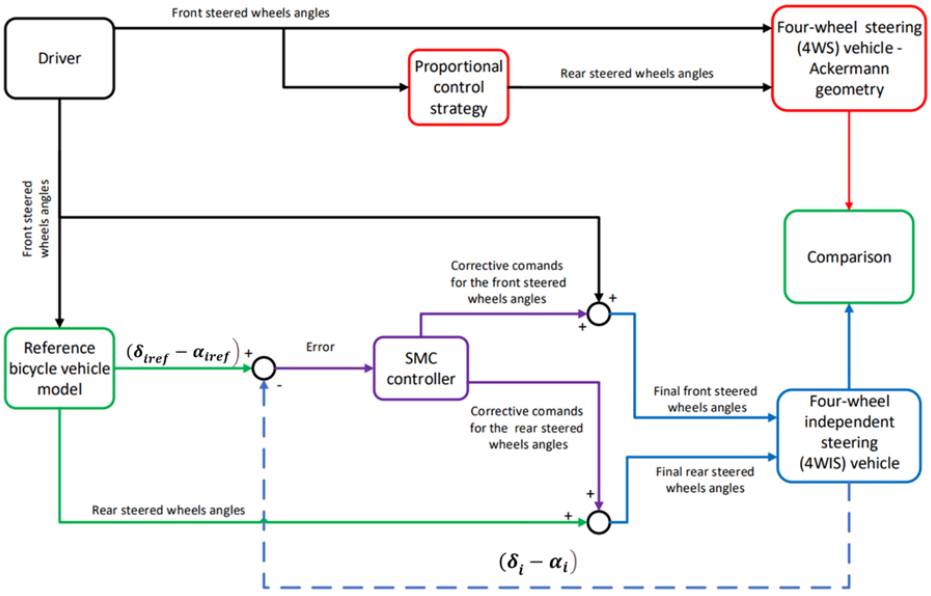

Fig. 1. Schematic overview of the presented concept

a) *Bicycle reference model*

As a reference model, a nonlinear all wheel steering (AWS) bicycle model (Figure 2) is used. The model has 2DOF, lateral velocity and yaw rate, while the longitudinal velocity is assumed to be constant. The tires are modelled using the Magic Tire Formula of Pacejka described by equations (1) and (2). Furthermore, the parameters of the reference model, 4WS and 4WIS vehicles are chosen to represent *C* vehicle segment as one of the most common vehicles. The vehicle parameters and the Pacejka model coefficients are presented in Table 1.

$$F_{yf} = D\sin\{C\arctan[B\alpha_f - E(B\alpha_f - \arctan(B\alpha_f))]\} \quad (1)$$

$$F_{yr} = D\sin\{C\arctan[B\alpha_r - E(B\alpha_r - \arctan(B\alpha_r))]\} \quad (2)$$

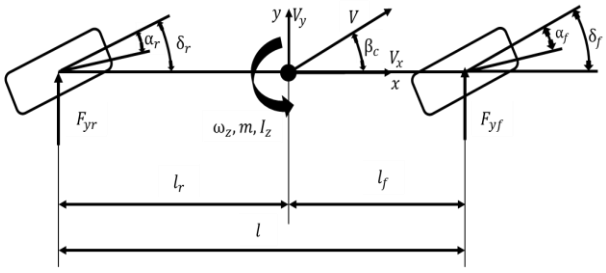

Fig. 2. 4WS bicycle vehicle model

Instead of 2WS bicycle model as a reference model, a 4WS was chosen since 2WS model has slower dynamic response and would force the 4WIS vehicle to mimic the performance of 2WS vehicle. These conclusions are presented in [8]. As, a control strategy for rear wheels, a linear control strategy is chosen which requires vehicle side-slip angle value of zero during the steady and transient state. Although the real value would never be zero, because a linear strategy is applied on a nonlinear model, nonetheless the performance of the reference model and the desired values are more favourable than some other strategies. The equations of the linear bicycle model, from which the strategy is derived, are presented in equations (3) and (4), while the control strategy itself is described by equation (5).

T a b l e 1

Vehicle bicycle model parameters

Mass (m):	1400 kg
Wheelbase (*l*):	2600 mm
Distance from centre of mass to front axle (l_f):	1200 mm
Inertia radius (iz):	1150 mm
Front wheel cornering stiffness $(C_{\alpha f})$:	50000 N/rad
Rear wheel cornering stiffness $(C_{\alpha r})$:	50000 N/rad
B	$C_{F\beta}/(CD)$
$C_{F\beta}$	$K_a \sin\left\{(2\arctan\left(\frac{F_n}{F_{nom}}\right)\right\}$
C	1.2
D	φF_n
E	0

$$\dot{V}_y = \left(\frac{-C_{\alpha f}-C_{\alpha r}}{mV_x}\right)V_y + \left(\frac{C_{\alpha r}l_r - C_{\alpha f}l_f}{mV_x} - V_x\right)\omega_z + \frac{C_{\alpha f}}{m}\delta_f + \frac{C_{\alpha r}}{m}\delta_r \quad (3)$$

$$\dot{\omega}_z = \left(\frac{C_{\alpha r}l_r - C_{\alpha f}l_f}{I_z V_x}\right)V_y + \left(\frac{-C_{\alpha f}{l_f}^2 - C_{\alpha r}{l_r}^2}{I_z V_x}\right)\omega_z + \frac{C_{\alpha f}l_f}{I_z}\delta_f - \frac{C_{\alpha r}l_r}{I_z}\delta_r \quad (4)$$

$$\delta_r = -\frac{C_{\alpha f}}{C_{\alpha r}}\delta_f + \frac{mV_x^2 + C_{\alpha f}l_f - C_{\alpha r}l_r}{C_{\alpha r}V_x}\omega_z \quad (5)$$

b) *Four-wheel steering (4WS) model using Ackermann geometry with proportional control strategy*

Figure 3 presents the Ackermann geometry of one axle. The 4WS vehicle is modelled to have identical front and rear axle, with the same geometry, the only difference being the maximum steer angle of the wheels of the front and rear axle.

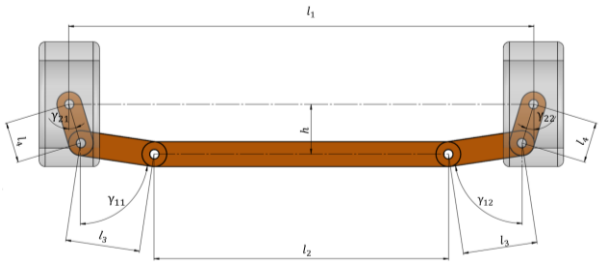

Fig. 3. 4WS vehicle's front and rear axle

For this vehicle, a proportional control algorithm is chosen and presented in equation (6), as one of simplest control strategies, combined with input delay of 0.1s in the rear wheels reaction. This delay is implemented to gain faster response from the vehicle.

$$\delta_r = K\delta_f \quad (6)$$

where $K = 0.2$. The relation between the inner and outer wheel is presented by equations (7) and (8). While it must be pointed out that the parameters of the vehicle are identical with the ones of the reference vehicle, except for the tire cornering stiffness which is assumed to be half the size of the cornering stiffness of the bicycle model. The Ackermann's geometry parameters are presented in Table 2. The values for the front and rear axle are identical.

$$\delta_{fo} = \gamma_{22f} - \arcsin\left(\frac{l_{1f} - l_{2f} - l_{3f}\sin(\gamma_{11f}) - l_{3f}\sin(\gamma_{12f}) + l_{4f}\sin(\gamma_{21f} + \delta_{fi})}{l_{4f}}\right) \quad (7)$$

$$\delta_{ro} = \gamma_{22r} - \arcsin\left(\frac{l_{1r} - l_{2r} - l_{3r}\sin(\gamma_{11r}) - l_{3r}\sin(\gamma_{12r}) + l_{4r}\sin(\gamma_{21r} + \delta_{ri})}{l_{4r}}\right) \quad (8)$$

T a b l e 2

Ackermann geometry – parameters

l_1:	1500 mm
l_2:	950 mm
l_3:	240 mm
l_4:	130 mm
h:	160 mm
$\gamma_{11}, \gamma_{12},$ (in straight ahead wheel position):	81.48°
$\gamma_{21}, \gamma_{22},$ (in straight ahead wheel position):	16.84°

In Figure 4 the turning process of the 4 WS vehicle is presented during higher velocity motion. Assuming only the steering angles of the wheels, orthogonal lines are drawn from the front wheels that intersect in point O_f and in the same way the orthogonal lines relative to the rear wheels intersect in Or. The values R_f and R_r represent the distances between the corresponding centre points and the vehicle's centre of mass. The value D_R represents the distance between those points. It must be pointed out when wheels side-slip angles are considered, the vehicle has single instantaneous centre of rotation. It's location is found in the distance between the points O_f and O_r. Smaller distance D_R means more precise positioning of instantaneous centre of rotation, while the vehicle's off- tracking, tire wear and tendency to stability loss would all be lower.

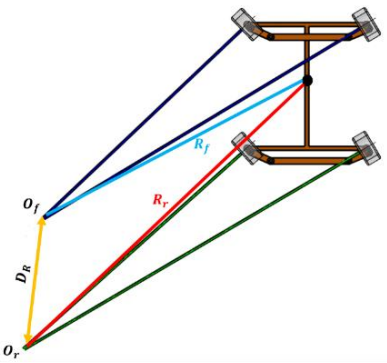

Fig. 4. Existence of two instantaneous centres of rotation using mechanical linkage of the front and the rear wheels

c) *Four-wheel independent steering (4WIS) model*

Last of the presented vehicle models is the 4WIS model (Figure 5). The vehicle has 4 wheels which can be steered independently. The input signal for the front wheels is the front wheel steering angle of the reference vehicle bicycle model. Afterwards, that value is modified using equations (9) and (10), in order to achieve the desired single instantaneous centre of rotation. Equation (9a) is derived from Figure 5 using triangle O12, while using triangle O34 equation (9b) is derived with assumption that the wheels' side-slip angles are negligible. By combining (9a) and (9b), the value of the inner front wheel steering angle is derived in eq. (10a). With the same approach, equation (10b) and rear wheels steering angles (11a and 11b) are derived.

$$\tan(\delta_{fef}) = a/d \tag{9a}$$

$$\tan(\delta_{fi}) = a/d_i \tag{9b}$$

$$\delta_{fi} = arctan\left(\frac{d}{d_i}\tan(\delta_{fref})\right); \tag{10a}$$

$$\delta_{fo} = arctan\left(\frac{d}{d_o}\tan(\delta_{fref})\right) \tag{10b}$$

$$\delta_{ri} = arctan\left(\frac{d}{d_i}\tan(\delta_{rref})\right); \tag{11a}$$

$$\delta_{ro} = arctan\left(\frac{d}{d_o}\tan(\delta_{rref})\right). \tag{11b}$$

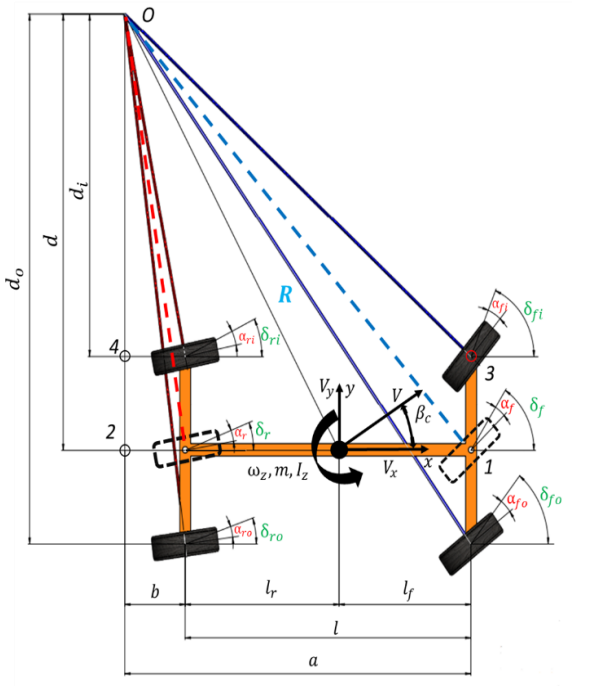

Fig. 5. 4WIS vehicle model

The variable d is obtained from the driver's command of the vehicle bicycle model and together with the values for d_i and d_o are calculated during the simulation in each integration step.

The wheel side-slip angles are taken into consideration in the SMC controllers which correct the driver's command. There, the real values of the parameters d, d_i and d_o and the turning radius are also calculated during the simulation in each integration step, but they are obtained from the 4WIS model. Those relations are presented in equations (12) and (13) and are used for the calculation of the value D_R.

$$\tan(\delta_{fj} - \alpha_{fj}) = \frac{a}{d_{4WIS}};\ \tan(\delta_{rj} - \alpha_{rj}) = \frac{b}{d_{4WIS}} \tag{12}$$

$$R = \sqrt{x^2 + (l_r + b)^2} \tag{13}$$

At the end, the wheel steering angles are corrected based on the error between the reference value from the bicycle model and the actual value of the 4WIS vehicle model. The values that are compared represent a difference between the steering angles of the wheels and the wheels' side-slip angles. Those values were chosen for the sliding mode control because in practice the traveling direction of the vehicle is determined by the difference between the wheel steering angles and the wheels side-slip angles, due to the lateral deformation of the tires.

The front and rear wheels side-slip angles of the four-wheel vehicle model are presented in equations (14) and (15). Also, these equations are used to calculate the desired reference values of the bicycle model.

$$\alpha_{fi} = \delta_{fi} - \frac{V_y - l_f\omega_z}{V_x - 0.5b_f\omega_z};\ \alpha_{fo} = \delta_{fo} - \frac{V_y - l_f\omega_z}{V_x + 0.5b_f\omega_z} \tag{14}$$

$$\alpha_{ri} = \delta_{ri} - \frac{V_y - l_r\omega_z}{V_x - 0.5b_r\omega_z};\ \alpha_{ro} = \delta_{ro} - \frac{V_y - l_r\omega_z}{V_x + 0.5b_r\omega_z} \tag{15}$$

The control strategy of SMC controllers is presented in the next section, while the comparison between the 4WS and 4WIS is presented in the results section.

It is important to mention that in both two-track vehicle models, the vertical load distribution of the wheels is taken into account. This distribution is calculated using equations (16) and (17) and it is used in Pacejka tire models.

$$F_{zfo} = \frac{0.5mgl_r}{l} + \frac{0.5ma_yh_c}{b_f} \tag{16a}$$

$$F_{zfi} = \frac{0.5mgl_r}{l} - \frac{0.5ma_yh_c}{b_f} \tag{16b}$$

$$F_{zro} = \frac{0.5mgl_f}{l} + \frac{0.5ma_y h_c}{b_r} \quad (17a)$$

$$F_{zri} = \frac{0.5mgl_f}{l} + \frac{0.5ma_y h_c}{b_r} \quad (17b)$$

3. DESIGN OF THE SLIDING MODE CONTROLLERS IN THE 4WIS MODEL

For the sliding mode control the sliding surface is defined by equation (18), while as mentioned above, the error is defined as subtraction between the actual and the reference value of the difference between the wheels' steering angle and the wheel side-slip angles (19). The control output, which is responsible for the final steering angle of the wheel is not solely dependent on the output command of the SMC (20), but also depends on the commands given by the driver. By combining equations (10), (11) and (20) the final values for the wheels' steering angles are calculated using equations 21 (21a and 21b) and 22 (22a and 22b).

$$s_j = \dot{e} + \lambda e \quad (18)$$

$$e_j = (\delta_{jref} - \alpha_{jref}) - (\delta_j - \alpha_j) \quad (19)$$

$$u_j = k\tanh\left(\frac{e_j}{\phi}\right) + u_{eq} \quad (20)$$

where $k = 1$, while $\phi = 10$, $\lambda = 50$ and $u_{eq} = 0$.

The values are chosen on basis of several conducted simulations.

$$\delta_{fi} = arctan\left(\frac{d}{d_i}\tan(\delta_{fref})\right) + k\tanh\left(\frac{e_{fi}}{\phi}\right); \quad (21a)$$

$$\delta_{fo} = arctan\left(\frac{d}{d_o}\tan(\delta_{fref})\right) + k\tanh\left(\frac{e_{fo}}{\phi}\right). \quad (21b)$$

$$\delta_{ri} = arctan\left(\frac{d}{d_i}\tan(\delta_{rref})\right) + k\tanh\left(\frac{e_{ri}}{\phi}\right); \quad (22a)$$

$$\delta_{ri} = arctan\left(\frac{d}{d_o}\tan(\delta_{rref})\right) + k\tanh\left(\frac{e_{ro}}{\phi}\right). \quad (22b)$$

4. SIMULATED MANOEUVRES AND RESULT ANALYSIS

Vehicles were tested using two manoeuvres described in the Standard ISO 7401. For the cornering manoeuvre, both vehicles are steered to achieve 4 m/s^2 of lateral acceleration in steady state, as requested by the standard, while traveling with constant longitudinal speed of 80 km/h. As recommended by the standard, the vehicles are tested for the step-steer and the single lane change manoeuvre. The road surface has friction coefficient of φ = 0.6.

The following comparative results of the 4WS and 4WIS vehicles are presented: steering angles, wheels' side-slip angles, lateral acceleration, yaw rate, vehicle side-slip angles, trajectory and radius error.

Step-steer

In the first manoeuvre, the different values of the steering angles of the 4WS and 4WIS can be observed in Figures 6 and 7, which also results in different wheels' side-slip angles presented in Figures 8 and 9. Lower values of wheel side-slip angles for the 4WIS vehicle indicate higher capability of the vehicle to withstand lateral forces.

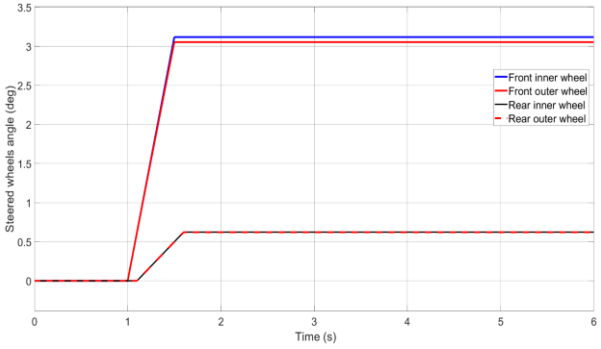

Fig. 6. Front and rear wheels' steering angles – 4WS vehicle

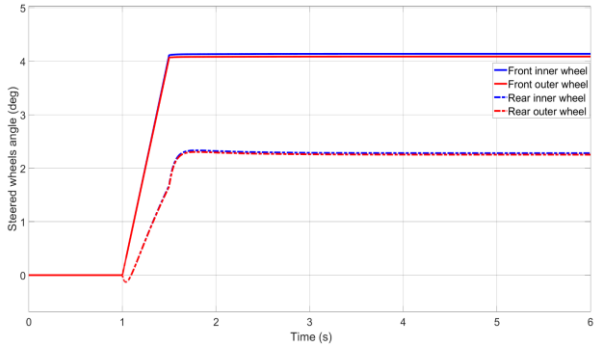

Fig. 7. Front and rear wheels' steering angles – 4WIS vehicle

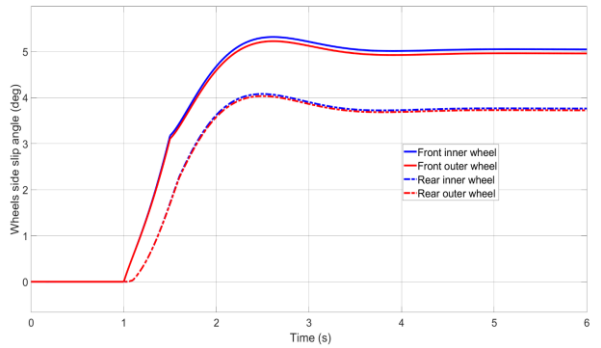

Fig. 8. Wheels' side slip angle – 4WS vehicle

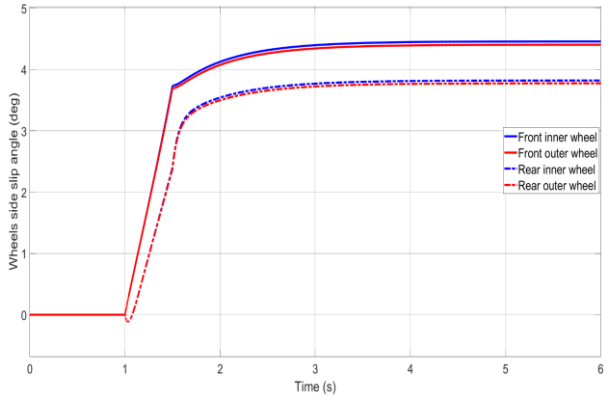

Fig. 9. Wheels' side slip angle – 4WIS vehicle

In the Figure 10, the value of the lateral acceleration is 4 m/s^2 in steady state, thus fulfilling the Standard ISO 7401. Also, it can be observed that the 4WIS has faster response than the 4WS vehicle. The same conclusion can be derived from Figure 11 with regard to the yaw rate, where the 4WIS reaches steady state after 1.5 seconds of the manoeuvre, just after driver's command reaches maximum value, while the 4WS settles after the 4th second.

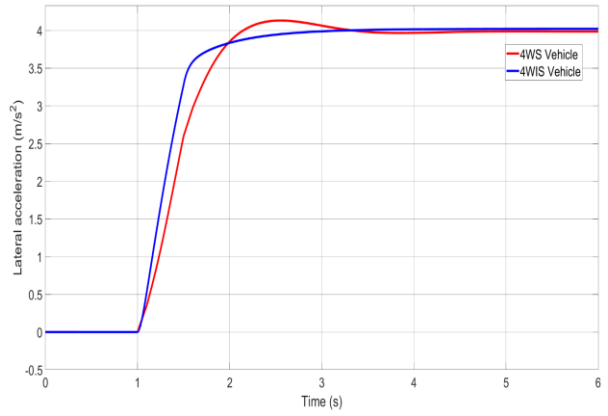

Fig. 10. Lateral acceleration

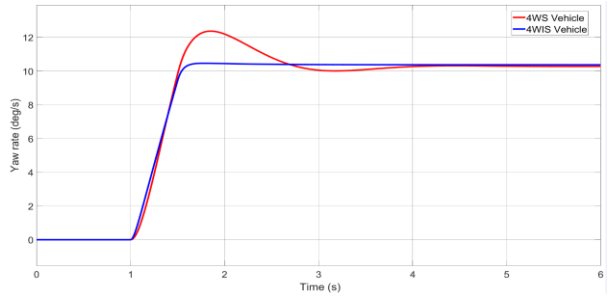

Fig. 11. Yaw rate

The biggest advantage of the proposed strategy can be noticed in the values for the vehicles side-slip angle (Figure 12), where the 4WIS achieves significantly smaller values. Therefore, it allows better driver perception and handling and increased safety. Because of the identical values of the lateral acceleration and yaw rate, the trajectory is almost identical (Figure 13). In Figure 14 the D_R parameter value is shown, where it can be observed that more than 30 mm in the transient period of the 4WS, while 4WIS possess value of approximately 3 mm. These small values are result of the smaller values of the steering angles of the wheels.

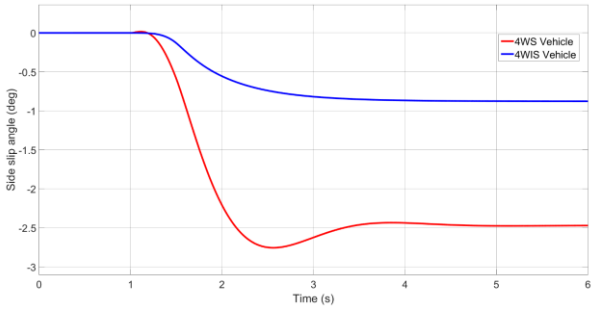

Fig. 12. Vehicle side slip angle

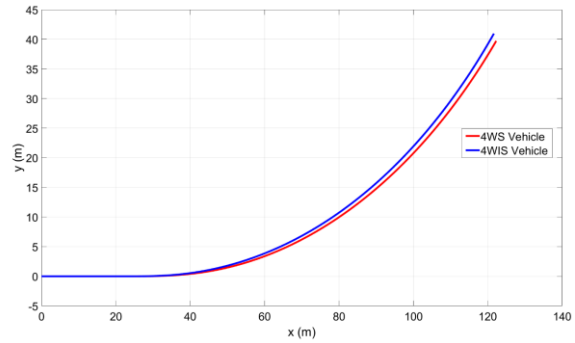

Fig. 13. Trajectory

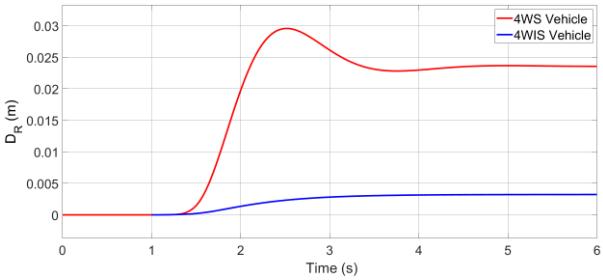

Fig. 14. D_R parameter

Single lane change

In this manoeuvre, vehicles are traveling with constant longitudinal velocity of 80 km/h and the steering angles of the wheels are assigned values so that (Figures 15 and 16) the vehicles achieve 4 m/s^2 of lateral acceleration in the first peak. Because of

the rear wheels control strategy of the 4WIS, they are turned in opposite direction at the beginning of the manoeuvre, therefore resulting in faster vehicle response (Figure 16).

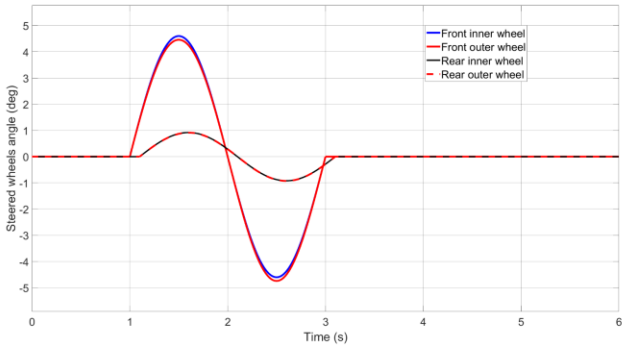

Fig. 15. Front and rear wheels steering angles – 4WS vehicle

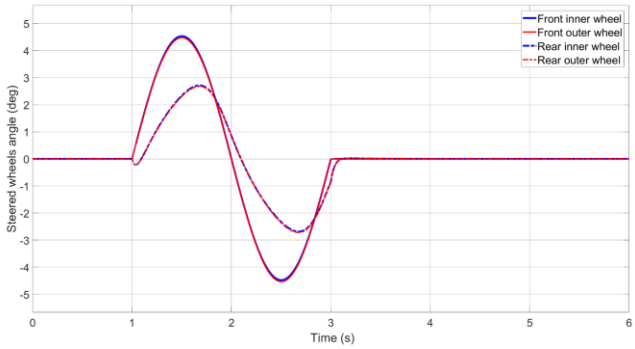

Fig. 16. Front and rear wheels steering angles - 4WIS vehicle

By observing the wheel side-slip angles (Figures 17 and 18), it can be concluded that at certain period of the manoeuvre, just before the 2nd second, the absolute values of the rear wheels side slip angles are larger than the front ones. That trend changes during the manoeuvre and the difference and the peaks are higher for the 4WS vehicle, but nevertheless, it results in a short transient period where both vehicles are showing oversteer characteristics. This period is much shorter for the 4WIS vehicle.

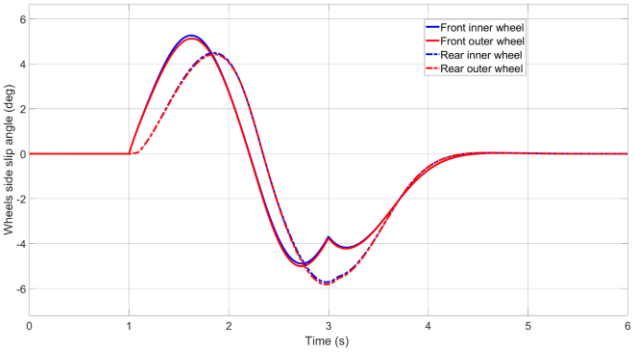

Fig. 17. Wheels side slip angle – 4WS vehicle

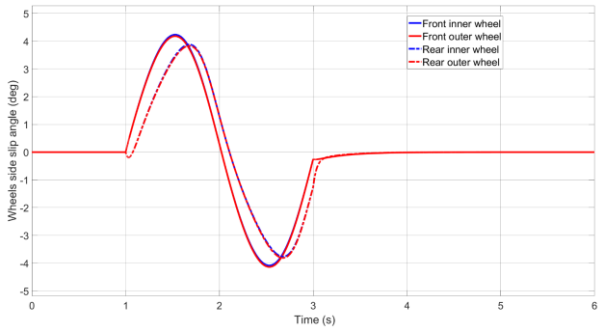

Fig. 18. Wheels side slip angle – 4WIS vehicle

This behaviour and the larger differences between the values of the rear and front wheel side-slip angles, results in requirement for longer time for the 4WS to reach steady state, around 5th second (Figure 19), while the maximum values of yaw rate (Figure 20) and side-slip angle (Figure 21) are larger, resulting in increased possibility for vehicle destabilization and deteriorated driver's perception of the vehicle's travelling direction.

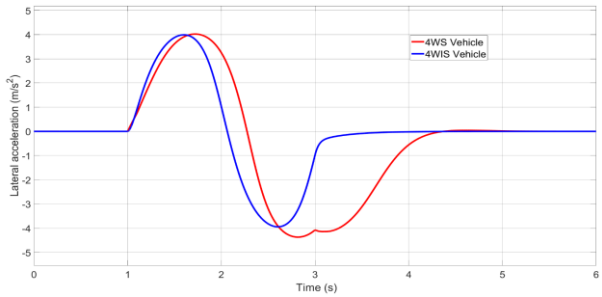

Fig. 19. Lateral acceleration

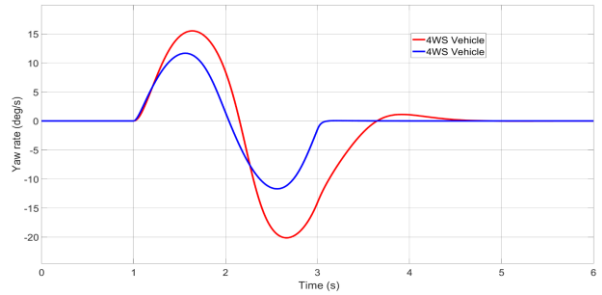

Fig. 20. Yaw rate

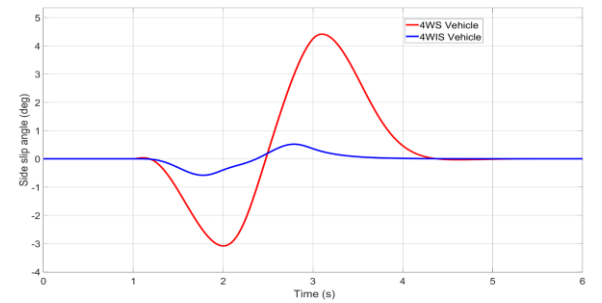

Fig. 21. Vehicle side slip angle

All of this can be confirmed with Figure 22, where the 4WS vehicle needs larger space to complete the manoeuvre (almost 4 meters) and the vehicle is moving in a direction much different than the initial lane. It must be pointed out that in real case scenario the driver would try to correct the vehicle's trajectory, thus avoiding traveling in the wrong lane and direction. In this situation the value of the D_R parameter (Figure 23) is almost 80 mm for the 4WS vehicle, while the 4WIS achieves value near to zero, having virtually single centre of rotation.

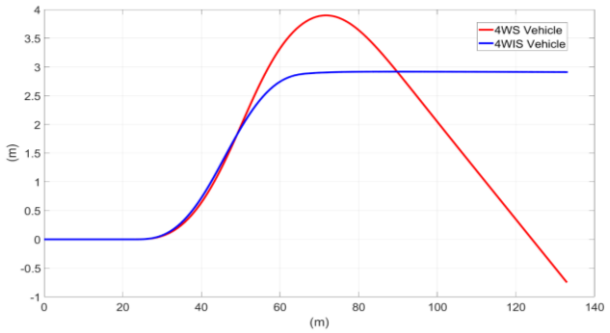

Fig. 22. Trajectory

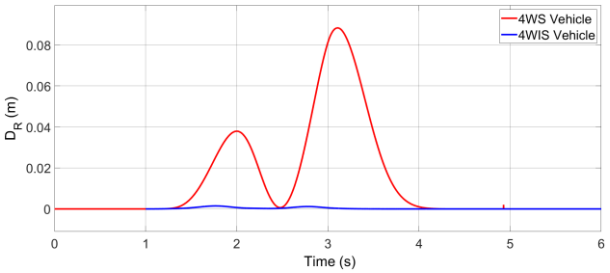

Fig. 23. D_R parameter

Single lane change – slippery road conditions

The previous results have shown better vehicle dynamic response and stability of the 4WIS vehicle over the 4WS. To further test the capabilities of the concept, tests were simulated in a case scenario of a single lane change, but the road conditions are deteriorated. Now the vehicles travel on a snow road surface with friction coefficient of $\varphi = 0.3$.

Results show that both vehicles would lose their stability in a step-steer manoeuvre because the driver's command remains constant throughout the manoeuvre, while during the single lane change the 4WIS controllers manage to prevent the vehicle from swirling out. Because of this, only the results of the single lane change manoeuvre are presented.

Figure 24 presents the steering angles of the wheels of the 4WIS vehicle, while the steering angles of the wheels for the 4WS are identical as those in Figure 15. While the front steered wheels angles are turned in similar angles like in the previous simulation, the rear steered wheels angles turn with higher intensity and are commanded with phase delay. The biggest contribution for this is SMC controllers attempting to prevent vehicle destabilization. The first indications of that and 4WS vehicle destabilization can be observed in Figure 25 and 26, where the wheels side-slip angles values of the 4WS are larger with tendency to further increase their value.

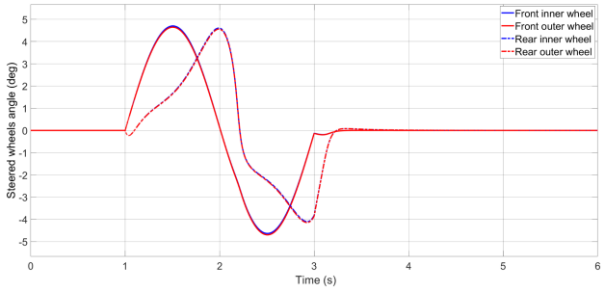

Fig. 24. Front and rear steered wheels angle – 4WIS vehicle

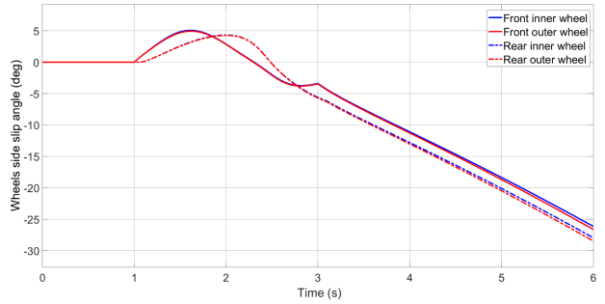

Fig. 25. Wheels side slip angle – 4WS vehicle

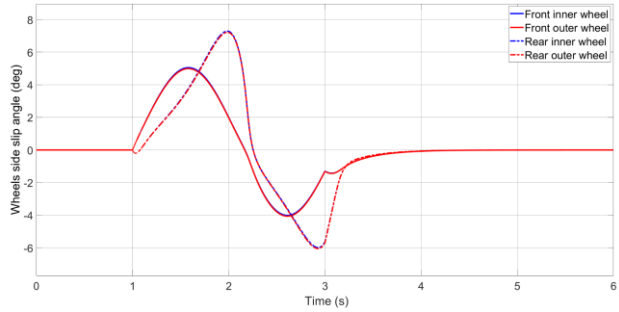

Fig. 26. Wheels side slip angle – 4WIS vehicle

The same conclusion can be drawn from Figures 27, 28 and 29 where the 4WS vehicle clearly fails to complete the manoeuvre, because the 4WS outputs don't follow sinusoidal form and don't reach steady-state value of 0. This can be only confirmed in Figure 30, where the trajectory of the 4WS shows that the vehicle starts to swerve, reaching total road width of around 10 m which is higher than

most of the standard highway lanes. Due to the larger values of the wheels side slip angles, the value D_R of the 4WS is more than fifty times higher than in the previous manoeuvre (Figure 31), resulting in larger vehicle off-tracking and tire wear and loads. On the other side the 4WIS maintains almost ideally single centre of rotation even though the vehicle is struggling to remain stable.

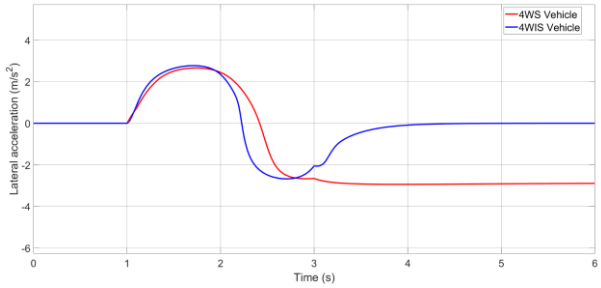

Fig. 27. Lateral acceleration

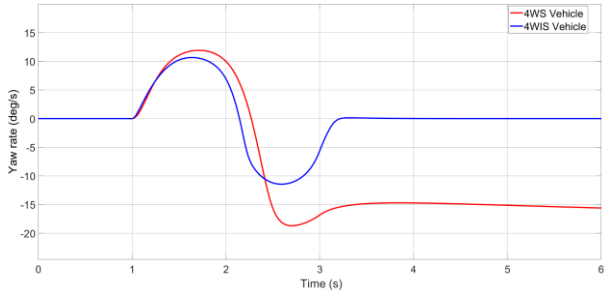

Fig. 28. Yaw rate

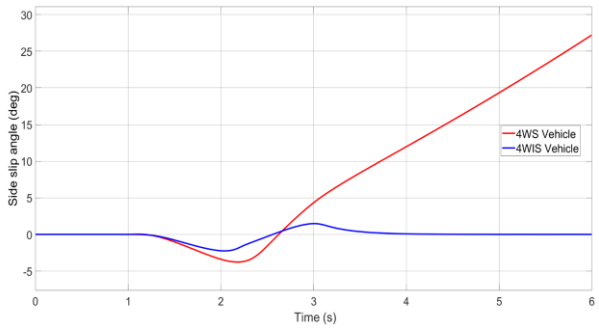

Fig. 29. Vehicle side slip angle

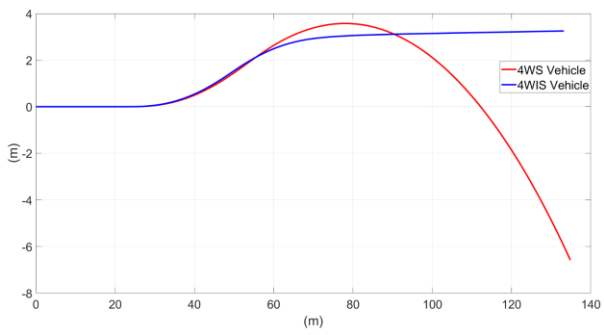

Fig. 30. Trajectory

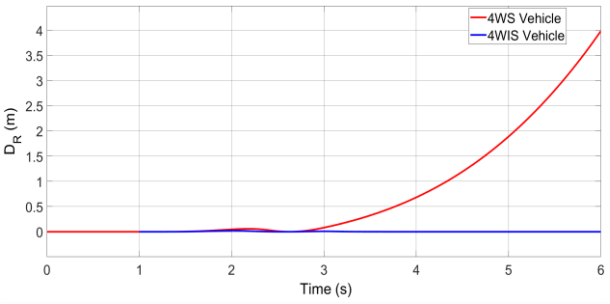

Fig. 31. D_R parameter

5. DISCUSSION AND CONCLUSIONS

The presented concept of a 4WIS vehicle had shown great potential over the 4WS vehicle. Faster vehicle response, shorter settling time and smaller vehicle side-slip angle which allows improved driver's evaluation and estimation of the vehicle traveling direction, are few of the improvements that this proposed control algorithm achieves. By conducting the same manoeuvre on a deteriorated road condition, the 4WIS manages to stabilize the vehicle while maintaining the value of the D_R almost to zero.

Implementation of SMC controllers in the 4WIS vehicle, that correct the error difference between the steering angles of the wheels and wheels side-slip angles is successfully used in the steer-by-wire steering concept that offers increased vehicle stability as well as improved handling and safety. Combined with the single instantaneous centre of rotation that this vehicle has, it results in decreased tire loads, wear and off-tracking.

With regard to the approximations made for this vehicle models, for the future work an improved vehicle model with more DOF or virtual vehicle model is planned, upgraded with additional active vehicle control systems.

REFERENCES

[1] Jordanoska, V.; Danev.; D.; Changoski, V. (2021): Evaluating coordinated cooperative control of three active car systems using fuzzy-logic, *IOP Conference Series: Materials Science and Engineering*, Vol. **1190** (1).

[2] Feng, J.; Chen, S.; Qi, Z. (2020): Coordinated chassis control of 4WD vehicles utilizing differential braking, traction distribution and active front steering, *IEEE Access***,** Vol. **8.** DOI: 10.1109/ACCESS.2020.2990729.

[3] Doumiati, M.; Sename, O.; Dugard L.; Martinez-Molina, J.; Gaspar, P.; Szabo, Z. (2023): Integrated vehicle dynamics control via coordination of active front steering and rear braking, *European Journal of Control*, Vol. **19**, Issue 2, pp. 121–143.

[4] Falcone, P.; Tseng, E. H.; Borrelli, F.; Asgari, J.; Hrovat, D. (2008): MPC-based yaw and lateral stabilisation via active front steering and braking, *Vehicle System Dynamics*, Vol. **46**, Issue sup 1, pp. 611–628.

[5] Ding, S.; Liu, L.; Park, Ju. (2019): A novel adaptive nonsingular terminal sliding mode controller design and its application to active front steering system, *International Journal of Robust and Nonlinear Control*, Vol. **29**, Issue 12.

[6] Zhang, J.; Wang, H.; Ma, M.; Yu, M.; Yazdani, A.; Chen, L. (2020): Active front steering-based electronic stability control for steer-by-wire vehicles via terminal sliding mode and extreme learning machine, *IEEE Transactions on Vehicular Technology*, Vol. **69**, Issue 12, pp. 14713–14726.

[7] Huang, W.; Wong, P. K.; Wong, K. I.; Vong, C. M.; Zhao, J. (2019): Adaptive neural control of vehicle yaw stability with active front steering using an improved random projection neural network, *Vehicle System Dynamics*, Vol. **59**, Issue 3.

[8] Changoski, V.; Gjurkov, I.; Jordanoska, V. (2022): Improving vehicle dynamics employing individual and coordinated sliding mode control in vehicle stability, active front wheel steering and active rear wheel steering systems in co-simulation environment, *IOP Conference Series: Materials Science and Engineering*, vol. **1271**.

[9] Hiraoka, T.; Nishihara, O.; Kumamoto, H. (2004): Model following sliding mode control for active four-wheel steering vehicle, *Review of Automotive Engineering*, Vol. **25**, pp. 305–313.

[10] Ferrara, A. (2017): *Sliding Mode Control of Vehicle Dynamics*, The Institution of Engineering and Technology, London.

[11] Chen, H.; Chen, S.; Zhou, R.; Huang, X.; Zhu, S. (2020): Research on four-wheel independent steering intelligent control strategy based on minimum load, *Concurrency and Computation: Practice and Experience*, Vol. **33**, Issue 9.

[12] Chen, X.; Han, Y.; Hang, P. (2020): Researches on 4WIS-4WID stability with LQR coordinated 4WS and DYC, *IAVSD 2019: Advances in Dynamics of Vehicles on Roads and Tracks*, Lecture Notes in Mechanical Engineering. Springer.

[13] Hang, P.; Xia, X.; Chen, X. (2021): Handling stability advancement with 4WS and DYC coordinated control: A gain-scheduled robust control approach, *IEEE Transactions on Vehicular Technology*, Vol. **70**, Issue 4, pp. 3164 –3174.

[14] Choi, M. W.; Park, J. S.; Lee, B. S.; Lee, M. H. (2008): The performance of independent wheels steering vehicle (4WS) applied Ackermann geometry, *2008 International Conference on Control, Automation and Systems*, Seoul, pp. 197–202.

[15] Oksanen, T.; Linkolehto, R. (2023): Control of four wheel steering using independent actuators, *IFAC Proceedings Volumes*, Vol. **46**, Issue 18, pp. 159–163.

[16] Liu, C.; Weichao Sun, W.; Zhang, J. (2020): Adaptive sliding mode control for 4-wheel SBW system with Ackermann geometry, *ISA Transactions*, Vol. **96**, pp. 103–115.

[17] Yim, S. (2020): Comparison among active front, front independent, 4-wheel and 4-wheel independent steering systems for vehicle stability control, *Electronics*, Vol. **9**, Issue 5.

[18] Nah, J.; Yim, S. (2020): Vehicle stability control with four-wheel independent braking, drive and steering on in-wheel motor-driven electric vehicles, *Electronics*, Vol. **9**, Issue 11.